Pak. J. Agri. Sci., Vol. 63(2), 493-500; 2026
ISSN (Print) 0552-9034, ISSN (Online) 2076-0906
DOI: 10.21162/PAKJAS/26.540
http://www.pakjas.com.pk

Evaluation of BSA-Derived Carbon Quantum Dots Against *Pectobacterium atrosepticum* for the Control of Potato Blackleg

Mohammad Umair Rafiq[1], Akhtar Hameed[1,*], Rana Binyamin[1], Muhammad Usman[2], Muhammad Faisal[3], Muhammad Waqar Alam[4], Waseem Hassan[5] and Subhan Ali[1]

[1]Department of Plant Pathology, MNS-University of Agriculture, Multan; [2]Department of Biochemistry and Biotechnology, MNS-University of Agriculture, Multan; [3]Institute of Plant Breeding and Biotechnology, MNS-University of Agriculture, Multan; [4]Department of Botany, University of Okara; [5]Department of Soil & Environmental Science, MNS-University of Agriculture, Multan
[*]Corresponding author's e-mail: akhtar.hameed@mnsuam.edu.pk

Pectobacterium atrosepticum (Pa), the causal agent of blackleg of potato (*Solanum tuberosum*), has been a severe threat to worldwide potato production. This study demonstrates the antimicrobial behaviour of carbon quantum dots (CQDs) prepared by using bovine serum albumin (BSA) as precursor through the acid hydrolysis method and coated with five different antibiotics to apply against *Pectobacterium atrosepticum* under *in-vitro* conditions. The *Pa* was cultured on NA media and confirmed through biochemical tests like potassium hydroxide (KOH), catalase test and gram stain. DNA sequencing further confirmed these isolates of *Pa* strains. The synthesized Bovine Serum Albumin-Carbon Quantum Dots (BSA-CQDs) were characterized by UV-visible trans-illuminator, dynamic light scattering (DLS), fourier transform infrared spectroscopy (FTIR) and transmission electron microscopy (TEM) analysis. The BSA-CQDs showed an intense blue colour, size of 2-3 nm, potential +27 mV, and functional groups -OH, -NH, C=C and C-O. Three concentrations were applied (300, 500, 700 ppm) in disk diffusion method and observed under time durations (24, 48 and 72 hours). The observed and recorded data revealed the best antibacterial behaviour of BSA-CQDs at 700 ppm, creating measurable inhibition zones (6.1 mm) after 72 hours. In the management trial, among the antibiotic-conjugated variants, BSA-CQDs coated with Ciprofloxacin and Kasugamycin showed the highest antimicrobial efficacy, producing the large inhibition zones average (9.93 mm and 9.04 mm, respectively) at 700 ppm after 72 hours of application, followed by Streptomycin (9 mm), Ampicillin (8.33 mm) and Oxytetracycline (7.43 mm). The research suggests that BSA-CQDs can serve as both antimicrobial agents and effective carriers for antibiotic delivery, ensuring targeted and sustained pathogen suppression. This study offers an eco-friendly and sustainable strategy to promote sustainable agriculture in pathogen-challenged cropping systems.

Keywords: Positively charged carbon quantum dots, potato, blackleg disease, antibacterial activity, bovine serum albumin, antibiotics

INTRODUCTION

Potato (*Solanum tuberosum* L.) is one of the most important food crops worldwide and plays a significant role in global food security. However, its production is severely affected by several bacterial diseases, among which blackleg caused by *Pectobacterium atrosepticum* is considered highly destructive. The pathogen infects stems and seed tubers, causing stem blackening, soft rot, wilting, and substantial yield losses under favorable environmental conditions (Zhang *et al*., 2024). Conventional disease management strategies, including crop rotation, use of healthy seed tubers, sanitation, and chemical bactericides have shown limited effectiveness due to environmental concerns, phytotoxicity, and the emergence of bacterial resistance (Shyntum *et al*., 2019; Weng *et al*., 2024). Therefore, the development of sustainable and effective alternatives for the management of potato blackleg is urgently needed.

In recent years, nanotechnology has emerged as a promising approach for plant disease management. Carbon quantum dots (CQDs) have been extensively studied as a nanomaterial due to their small size, surface reactivity, solubility in water, biocompatibility and antimicrobial activity (Kayani *et al*., 2024). In recent years, nanoscale carbon particles (nanocarbons) known as CQDs have been gaining traction as versatile tools in plant protection, owing to their tunable

Rafiq, M.U., A. Hameed, R. Binyamin, M. Usman, M. Faisal, M.W. Alam, W. Hassan and S. Ali. 2026. Evaluation of BSA-Derived Carbon Quantum Dots Against *Pectobacterium atrosepticum* for the Control of Potato Blackleg. Pakistan Journal of Agricultural Sciences 63:493-500.
[Received 14 Apr 2026; Accepted 20 Jun 2026; Published (online) 27 Jun 2026]

surface chemistry, high biocompatibility, and unique optical properties (Arshad *et al*., 2025). The antibacterial ability of CQDs and other nanoparticles has been shown in several plant pathogens via mechanisms like cell membrane disruption, generation of reactive oxygen species (ROS) and disruption of cellular metabolism (Wang *et al*., 2024). Moreover, CQDs have also been explored as carriers for antimicrobial compounds and drug delivery systems due to their high surface functionality and stability.

Nanoparticles have been tested against various *Pectobacterium* species; however, little information is available on the use of bovine serum albumin-derived carbon quantum dots (BSA-CQDs) against *Pectobacterium atrosepticum* in potato blackleg disease. In particular, the antibacterial efficacy of antibiotic-based BSA-CQDs against this pathogen remains largely unexplored.

Therefore, the present study was designed to synthesize and characterize BSA-derived CQDs and evaluate their antibacterial activity, alone and in combination with selected antibiotics, against *Pectobacterium atrosepticum* under in vitro conditions. The study hypothesized that antibiotic-based BSA-CQDs would exhibit enhanced antibacterial activity compared with BSA-CQDs alone and could serve as a potential nano-based strategy for sustainable management of potato blackleg.

MATERIALS AND METHODS

***Surveillance and Sample Collection*:** Potato fields in Multan were surveyed to collect samples showing typical symptoms of blackleg disease. Six fields were selected randomly, and disease incidence was recorded by counting the total number of plants and those exhibiting symptoms. Six representative samples were collected from each field using a random zig-zag pattern. To ensure traceability, GPS coordinates were recorded for each sampling site 30°13'03"N 71°38'37"E, 30°14'27"N 71°37'49"E, 30°17'25"N 71°44'59"E, 30°16'53"N 71°38'28"E, 30°13'35"N 71°38'00", 30°08'45"N 71°26'48"E (Figure 1). The collected samples were placed in labeled polythene bags under low-temperature conditions to minimize damage during transport and were brought to the Diagnostic Laboratory at MNS University of Agriculture, Multan, for isolation and analysis. For laboratory analysis, composite samples were prepared to represent the collected material.

***Isolation and Purification of Pectobacterium atrosepticum*:** Nutrient agar (NA) media (28 g/L; NaCl 5 g, peptone 5 g, beef extract 1 g, yeast extract 2 g, agar 15 g), was prepared in distilled water, sterilized at 121 °C and 15 psi for 30 minutes, and poured into sterilized petri plates (Kumar^1 *et al*., 2025). Infected tissues of leaves were cut along with some healthy parts, surface-sterilized with 1% NaOCl, rinsed completely with distilled water, dried and then placed on NA plates. Under controlled conditions, these plates were incubated, and bacterial growth was observed daily. Colonies were streaked repeatedly on fresh media to achieve a single uniform colony (Thakur, 2024).

***Identification of Pectobacterium atrosepticum*:** These isolates were identified as *P. atrosepticum* through different biochemical test like Gram staining, KOH test, and catalase test. In Gram staining, smears had been prepared, stained with crystal violet, iodine, ethanol, and safranin and examined under a microscope. Pink colour was appeared which confirmed the gram-negative nature (Hameed *et al*., 2024).

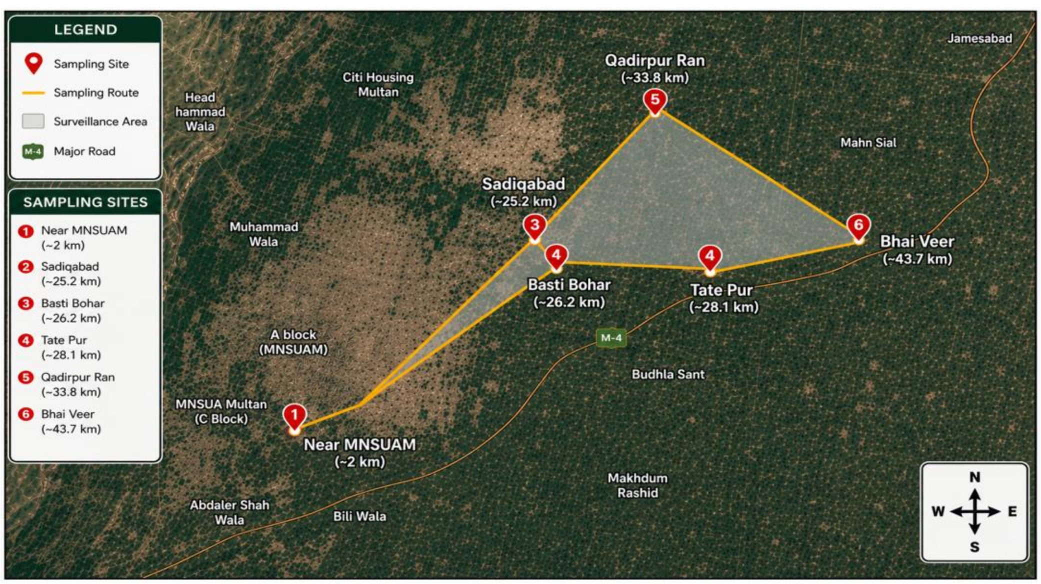

Figure 1. Map showing the sampling locations of potato fields infected with black leg disease.

The KOH test was performed by suspending colonies in 3% KOH, where string-like viscosity proved their gram-negative identity (Rodríguez-Parra *et al.*, 2022). Catalase activity was determined by mixing hydrogen peroxide with the culture; bubble formation indicated the enzymatic activity of bacteria (Hadwan *et al.*, 2024). Molecular confirmation of the pathogen was previously conducted through PCR amplification and sequencing of representative aggressive isolates. The obtained sequences were analyzed using BLAST and confirmed as *Pectobacterium atrosepticum*. Detailed molecular characterization procedures and sequence information have been reported by Hameed *et al*. (2024).

***Pathogenicity Test*:** Potato tuber assay was used to confirm the pathogenicity. To prepare the inoculum, colonies were grown on nutrient broth and shaken overnight at 28 °C to form a suspension, containing approximately 10^8 cfu/ml of bacteria, as confirmed by spectrophotometry. Surface-sterilized susceptible varieties of tubers were inoculated with 0.5 ml suspensions containing bacteria and maintained under humid chambers under a temperature range of 25 ± 2 °C. Infected tubers were observed for symptom development for 4-5 days after inoculation; thereafter, re-isolation of the bacterium was done as a confirmatory check for pathogenicity (Haque *et al.*, 2025). Pure cultures were preserved by suspending them in 50% glycerol (1:1 v/v) in Eppendorf tubes and stored at 4 °C after labeling (Yaish, 2024).

***CQDs Synthesis and Characterization*:** Carbon quantum dots (CQDs) were prepared using a precursor, bovine serum albumin (BSA) by acid hydrolysis. Briefly, 1 g of BSA was dissolved in 10 mL of Milli-Q water by adding 30 mL concentrated H_2SO_4 (95%) dropwise under constant stirring for 2.5 hours in a water bath at a constant temperature of 50 °C. Then the solution was neutralized to 7 pH by 2 M NaOH solution, dialyzed and purified using a 10 kDa Molecular Weight Cut-Off (MWCO) membrane to remove the residual salts and excess regents with the external Milli-Q water changed every 6 hours. The 10 kDa MWCO effectively retains the rigid, spherical 2-3 nm BSA-CQDs within the bag due to their dense structural geometry and the formation of a bulky surface hydration shell in an aqueous solution, while allowing smaller molecular precursors to pass through. This purification has been verified by checking the external dialysate water to ensure the pH was neutral (7.0) and that there was absolutely no residual fluorescence with a 365 nm UV lamp, which proves the complete removal of unreacted precursors and free chemical residues. Finally, the purified solution was lyophilized to obtain the CQDs (Usman *et al.*, 2020). The prepared CQDs were analyzed by some standard analytical methods. DLS and Zeta potential measurement (Zeta-sizer Ultra) were used for measuring size distribution as well as surface charge. UV-visible spectroscopy was used for determining absorption spectra and confirming fluorescent behavior. TEM was used for obtaining precise images of size, shape, as well as crystalline structure. FTIR was used for determining functional groups as well as bonding characteristics (Roostaee and Ranjbar-Karimi, 2025).

Five antibiotics; oxytetracycline, streptomycin, ampicillin, kasugamycin and ciprofloxacin, were absorbed onto the CQDs to define them as carriers of antibiotics. Equal volumes of antibiotic and CQDs solutions were vortexed and left at room temperature for 8 hours and then dialyzed with 10 kDa cutoff membranes to remove unbound molecules following the same verification protocol mentioned above (Marković *et al.*, 2024). Coating success was confirmed by UV-visible spectrophotometry, FTIR, DLS, and zeta potential analysis, showing spectra changes, presence of functional groups, and size and surface charge variation and proving antibiotic adsorption.

***Anti-bacterial Activity*:** The antimicrobial activity was assessed using the disk diffusion method (Balouiri *et al.*, 2016). Sterile 6 mm discs were placed on agar plates inoculated with test microorganisms. The concentration of 10µL of CQD discharged to the discs was 300 ppm, 500 ppm and 700 ppm. Sterile physiological saline buffer (0.9% NaCl) was used as the negative control and pure antibiotics were used as the positive benchmark control. Plates were incubated at 28–30 °C for 24–72 h. The diameter of the inhibition zone (mm) was measured after incubation at 24, 48 and 72 h to assess the time dependent antibacterial activity of CQDs and antibiotic-based CQDs (Mikhail *et al*., 2025).

***Statistical Analysis*:**

Data were analyzed using analysis of variance (ANOVA) under a completely randomized design (CRD) with three replications (Steel *et al*., 1997). Mean comparisons were performed using Tukey's HSD test at $P \leq 0.05$, and results are presented as mean ± SE.

RESULTS

***Isolation, Identification, and Pathogenicity Test*:** Potato plants exhibiting typical blackleg symptoms, including stem blackening, wilting, and soft rot, were collected from potato-growing fields in Multan (Figure 2A). Bacterial colonies isolated from infected tissues on nutrient agar were creamy-white, circular and smooth in texture (Figure 2B).

The biochemical characterization was used to confirm the isolates belonged to the Gram-negative group, with pink-stained cells during Gram staining and characteristic viscous thread formation during KOH test (Figure 2C–D). The presence of catalase activity was also confirmed by bubble formation following the addition of hydrogen peroxide (Figure 2E). These results confirmed the typical characteristics of *Pectobacterium atrosepticum*. The pathogen identity was also supported by previously published molecular characterization of the most aggressive isolates (PCA-5, PCA-7 and PCA-10). Sequence analysis and BLAST comparison confirmed their identity as *Pectobacterium atrosepticum*, and the corresponding sequences were deposited in GenBank under accession numbers MK392513.1, MK392518.1, and MK392519.1 (Hameed *et al.*, 2024).

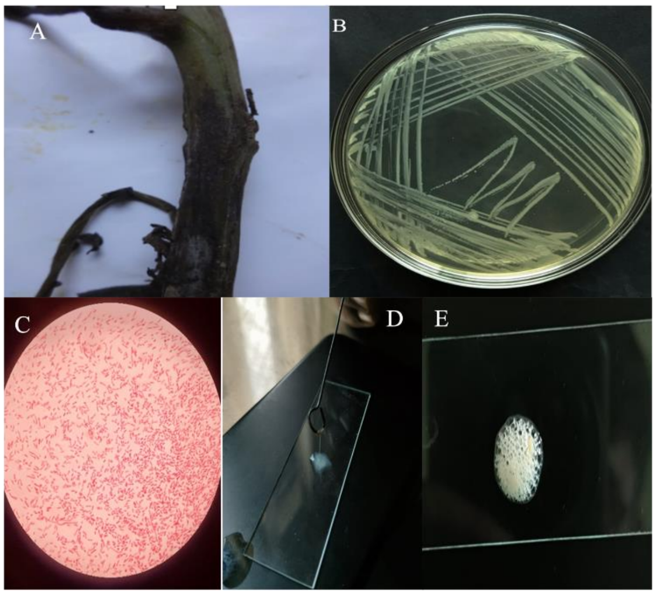

Figure 2. (A) Blackleg symptomatic plant collected from the infected field (B) Isolated pathogen on the NA media (C) Gram staining slide for the Pa (D) KOH slide showing a clear thread-like structure (E) Catalase test shows bubble formation that confirms catalase activity of Pa.

The pathogenicity assay confirmed the soft rot and maceration symptoms on potato tubers inoculated with the pathogen while healthy potato tubers were observed in the control (Figure 3). Re-isolation of the bacterium from infected tubers further confirmed the pathogenic nature of the isolate.

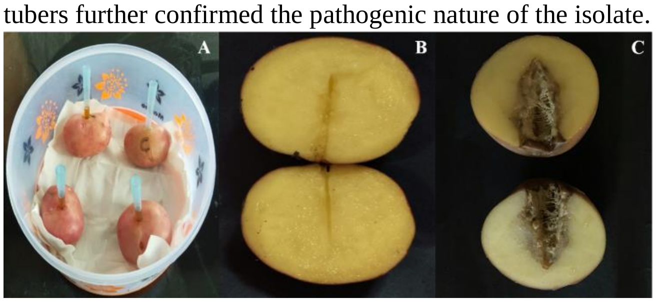

Figure 3. Pathogenicity Test; (A) Tuber Assay Method (B) Control potato with no symptoms (C) Decaying potato symptoms

***CQDs Synthesis and Characterization*:** The synthesized BSA derived carbon quantum dots (BSA-CQDs) exhibited strong blue fluorescence under UV illumination, indicating their fluorescent nature (Figure 4A–B). The analysis of the major functional groups by FTIR showed the presence of –OH, –NH, C=C and C–O groups, signifying the successful surface functionalization of the CQDs (Figure 4C).

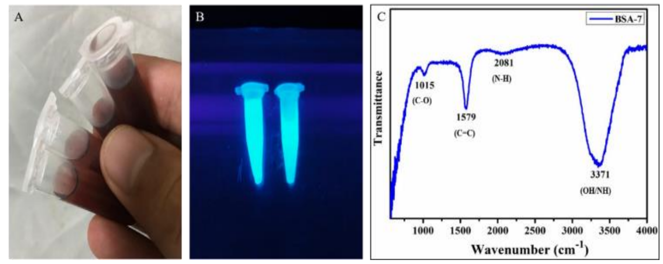

Figure 4. (A) BSA based CQDs (B) Exhibition off intense blue colour under UV light at UV trans-illuminator (C) Analysis of BSA based CQDs under FTIR between 500 cm^{-1}-4000 cm^{-1}.

The average particle size using dynamic light scattering (DLS) was 2.327 nm, and the surface charge using zeta potential was +27 mV (Figure 5A–B). TEM was also performed to show that the particles were spherical and had a size of 2–3 nm (Figure 5C), which agreed with the results from the XRD analysis. The characterization results showed that the BSA-CQDs were synthesized successfully with stable dimensions and surface properties.

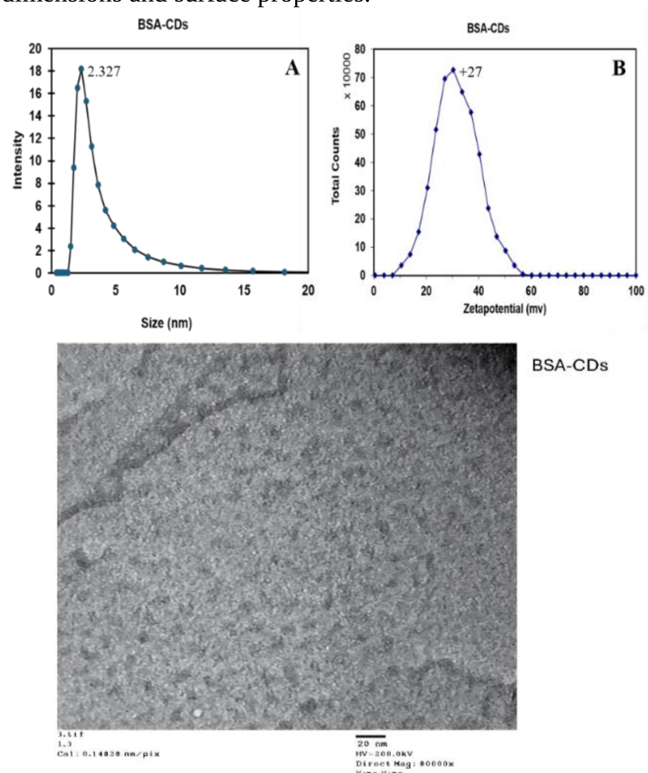

Figure 5. (A) DLS (B) Zeta-potential of BSA-CQDs showing size (2.327 nm) and potential positive charge (+27) respectively (C) TEM analysis showing the size of BSA-CQDs between 2-3 nm that confirm the size through DLS.

Antibiotic loading of CQDs: The synthesized BSA-CQDs were successfully fused with five antibiotics (ciprofloxacin, kasugamycin, ampicillin, oxytetracycline and streptomycin) for antimicrobial assessment. Comparative spectroscopic and particle characterization analyses showed spectral profile, particle size, and surface charge changes upon antibiotic association, confirming the successful interaction of antibiotics and BSA-CQDs.

Antibacterial Activity by Disc Diffusion Assay: The antibacterial activity of BSA-CQDs and antibiotic-conjugated BSA-CQDs against *Pectobacterium atrosepticum* was evaluated using the disc diffusion method. Clear inhibition zones were observed around treated discs, whereas the negative control showed no antibacterial activity. The inhibitory response increased with both concentration and incubation time, indicating a dose- and time-dependent antibacterial effect.

In-vitro evaluation of BSA-CQDs and CQDs as carrier of antibiotic for the management of Pectobacterium atrosepticum: BSA-CQDs alone exhibited moderate antibacterial activity against *P. atrosepticum*, producing an average inhibition zone of 5.29 mm. The antibacterial effect significantly increased after conjugation with antibiotics (Figure 6). Among all treatments, Ciprofloxacin-CQDs demonstrated the strongest antibacterial activity with the highest inhibition zone (9.08 mm), followed by Kasugamycin-CQDs (8.15 mm) and Streptomycin-CQDs (8.04 mm). Ampicillin-CQDs and Oxytetracycline-CQDs showed moderate inhibition zones of 7.37 mm and 6.65 mm, respectively, while the negative control showed no inhibition (Table 1; Figure 7).

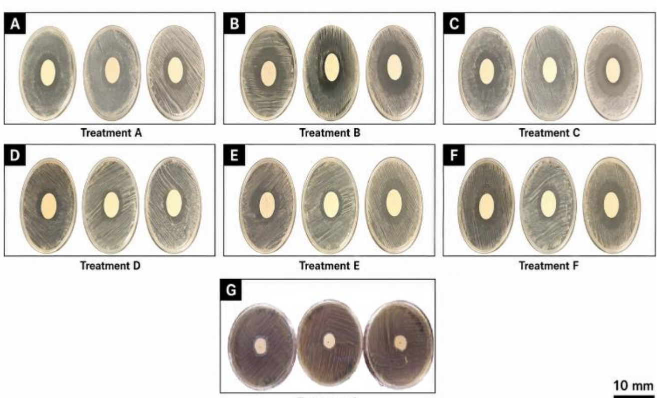

Figure 6. In-vitro management of *Pectobacterium atrosepticum* through BSA-CQDs and antibiotics-coated BSA-CQDs via disc diffusion method. Treatments are (A) BSA-CQDs, (B) Ciprofloxacin-CQDs, (C) Kasugamycin-CQDs, (D) Ampicillin-CQDs, (E) Oxytetracycline-CQDs, (F) Streptomycin-CQDs and (G) Control.

Table 1. Impact of BSA-CQDs in pure form and in combination with antibiotics on the development of *Pectobacterium atrosepticum*.

Sr.	Treatment	Inhibition zone (mm)
1	BSA-CQDs	5.29 d
2	Ciprofloxacin-CQDs (BSA-C)	9.08 a
3	Kasugamycin-CQDs (BSA-K)	8.15 ab
4	Ampicillin-CQDs (BSA-A)	7.37 bc
5	Oxytetracycline-CQDs (BSA-O)	6.65 c
6	Streptomycin-CQDs (BSA-S)	8.04 ab
7	Control (C)	0.00 e
HSD		**1.04**

Mean values significantly as determined by the HSD test ($P \leq 0.05$)

The interaction between treatment and concentration (TxC) revealed a concentration-dependent increase in antibacterial activity. Pure BSA-CQDs showed inhibition zones ranging from 4.8 mm at 300 ppm to 5.83 mm at 700 ppm. Similarly, all antibiotic-conjugated formulations exhibited enhanced inhibition with increasing concentrations. Ciprofloxacin-CQDs showed the highest antibacterial response, reaching 9.63 mm at 700 ppm, followed by Streptomycin-CQDs (8.8 mm) and Kasugamycin-CQDs (8.77 mm). Oxytetracycline-CQDs showed comparatively lower antibacterial activity among all tested formulations (Figure 8).

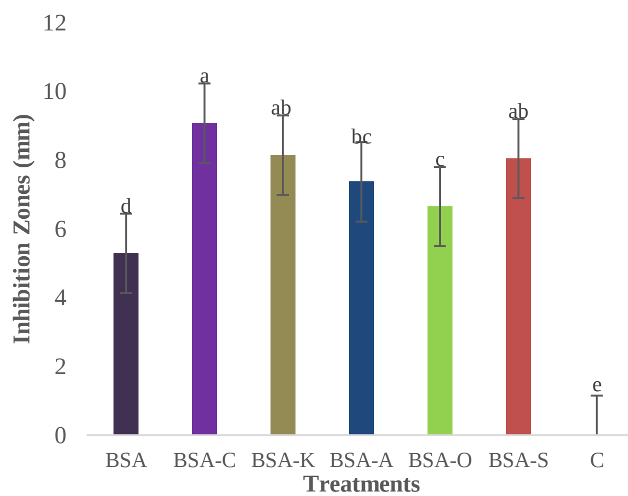

Figure 7. *In vitro* antibacterial activity of BSA-CQDs alone and antibiotic-conjugated BSA-CQDs against *Pectobacterium atrosepticum*. Bars represent mean inhibition zone (mm) ± SE (n = 3). Different letters indicate significant differences among treatments according to Tukey's HSD test ($P \leq 0.05$).

A time-dependent increase in antibacterial activity was also observed in the treatment × time (TxTi) interaction (Figure 9). Pure BSA-CQDs exhibited gradual inhibition zone enlargement from 4.5 mm at 24 h to 6.1 mm at 72 h (Figure

9). Among the conjugated formulations, Ciprofloxacin-CQDs remained the most effective treatment throughout the incubation period, producing inhibition zones of 8.16 mm, 9.13 mm, and 9.93 mm after 24, 48, and 72 h, respectively. Kasugamycin-CQDs and Streptomycin-CQDs also demonstrated strong antibacterial responses over time. No inhibition zones were observed in the negative control treatment at any observation interval.

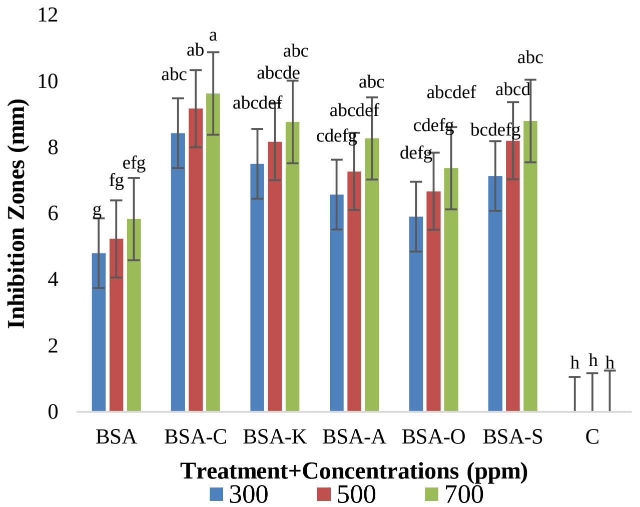

Figure 8. Effect of the interaction between treatments and concentrations (T × C) on the inhibition of *Pa*. Data are presented as mean inhibition zone (mm) ± SE (n = 3). Means were compared using two-way ANOVA followed by Tukey's HSD test (P ≤ 0.05). Different letters indicate significant differences among treatment × concentration combinations.

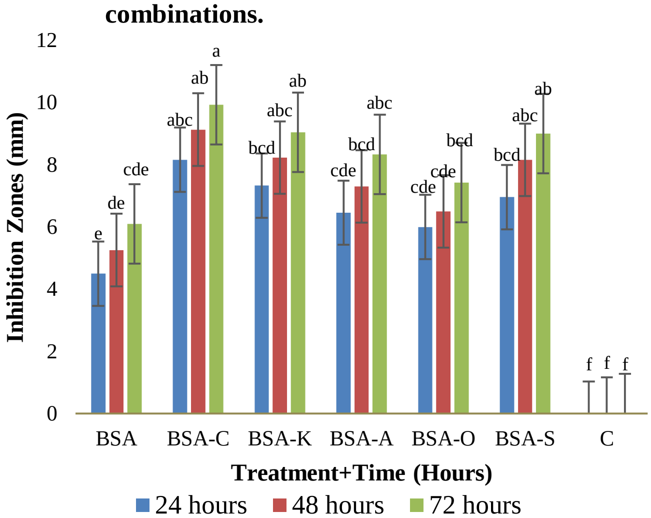

Figure 9. Effect of the interaction between treatments and incubation time (T × Ti) on the inhibition of *Pa*. Data are presented as mean inhibition zone (mm) ± SE (n = 3). Means were compared using two-way ANOVA followed by Tukey's HSD test (P ≤ 0.05). Different letters indicate significant differences among treatment × time combinations.

Overall, the results demonstrated that antibiotic-conjugated BSA-CQDs significantly enhanced antibacterial activity against *Pectobacterium atrosepticum*, with Ciprofloxacin-CQDs showing the most promising inhibitory effect under in-vitro conditions.

DISCUSSION

The study investigated the antibacterial effectiveness of directly applying BSA-CQDs and carbon quantum dots (CQDs) coated with five antibiotics: Ciprofloxacin, Kasugamycin, Ampicillin, Oxytetracycline, and Streptomycin at three concentrations (300, 500, and 700 ppm) against *Pectobacterium atrosepticum*, the bacterium causing potato blackleg. The results showed significant concentration-dependent antibacterial effects, with the largest inhibition zones seen at 700 ppm after 72 hours for all tested antibiotics. The BSA-CQDs produced inhibition zones of 6.1 mm, while among the antibiotics, Ciprofloxacin-coated CQDs had the strongest effect (9.93 mm), followed closely by Kasugamycin (9.04 mm). Oxytetracycline showed the least efficacy (7.43 mm at 700 ppm). These outcomes correlate with previous studies indicating a synergistic effect of nanomaterials and antibiotics. (Ton *et al.*, 2025) stated that antibiotic-functionalized CQDs significantly enhance antibacterial activity compared to antibiotics alone due to amplified membrane permeability and improved cellular interaction. The absorption method for conjugating antibiotics, as in this research, enables non-covalent binding, preserving the bioactivity of both CQDs and antibiotics that ensures high antimicrobial performance as discussed by (Aftab *et al.*, 2025) against human bacterial diseases.

The most active was the broad-spectrum fluoroquinolone antibiotic, Ciprofloxacin, which inhibits bacterial DNA gyrase and topoisomerase IV, enzymes that are crucial for DNA replication, transcription, and cell division. Conjugation with positively charged BSA-CQDs may have enhanced bacterial cell interaction and facilitated localized delivery of the antibiotic, thereby improving antibacterial efficacy against *Pectobacterium atrosepticum* (Pei *et al.*, 2025). Similarly, Kasugamycin-conjugated BSA-CQDs created significant inhibition zones, supporting the results by (Hu *et al.*, 2024), who described the kasugamycin-conjugated ZnO-QDs had boosted anti-microbial effects against rice blast because of their nano-sizes and positive surface charge. The increased inhibition zones based on concentration suggest that higher doses of antibiotic-coated CQDs boost antibacterial effectiveness. This correlates with the study by (Murei *et al.*, 2020) stated that increased concentration of ampicillin conjugated AgNPs suppresses microbial growth efficiently. Furthermore, the CQDs themselves express mild antibacterial behaviour because of ROS production, which disrupts bacterial cell walls and amplifies the damage when conjugated with antibiotics (Packialakshmi and Kim, 2025). Excitingly, Oxytetracycline conjugated CQDs exhibited limited effectiveness, possibly because of lower stability or affinity of antibiotics during the adsorption. It has been reported that antibiotics with weak binding to nanomaterials tend to release prematurely or degrade, resulting in reduced efficacy (Zhou *et al.*, 2024). Moreover, resistance mechanisms in *P. atrosepticum* strains may affect their sensitivity toward certain antibiotics. Based on the findings of this study, the use of antibiotic conjugated CQDs has great potential to be an effective and useful nano-biotechnological tool for controlling bacterial pathogens in agricultural applications. The outcomes are consistent with the worldwide development of hybrid nanotechnology-based antibiotics that tackle evolving bacterial resistance and enhance delivery systems (Dey *et al*., 2024).

The anti-bacterial properties of BSA derived CQDs and their antibiotic conjugates were seen in the current study against *P. atrosepticum*, but there are still many translation challenges. The large-scale production of CQDs with consistent surface reactivity, charge distribution and stability continues to be a significant limitation for field application. The rhizospheric environment consists of complex soil conditions, including aggregation of nanoparticles, availability of antibiotics, and possible effects on non-target soil organisms, which requires thorough assessment of CQD behavior in such environments. Future studies are needed to optimize nano-formulation parameters, understand the interactions between molecules and bacterial membranes and to evaluate in the field. The use of CQD-based nanomolecules in combination with biosensing and smart delivery systems could enable targeted and real-time pathogen management in distant future, protecting crop health.

***Conclusion*:** This research explores the antimicrobial capability of BSA-CQDs against *Pectobacterium atrosepticum*, the causative agent of potato blackleg. *Pa* isolates were successfully identified through biochemical assays and further validated by DNA sequencing. Synthesized BSA-CQDs (2–3 nm; +27 mV) demonstrated promising antimicrobial activity against *Pa*, highlighting their potential as an effective nano-antibacterial agent. BSA-CQDs exhibited strong antibacterial activity against *Pa*, with the highest inhibition observed at 700 ppm after 72 hours. Antibiotic-conjugated BSA-CQDs, particularly those coated with ciprofloxacin and kasugamycin, further enhanced pathogen suppression, highlighting their potential as sustainable nano-carriers for targeted disease management in agriculture.

***Conflict of interest*:** No conflicts of interest have been disclosed by the authors.

Authors' contribution: MU Rafiq: conceptualization, investigation, CQD synthesis, characterization, *in-vitro* testing and original draft. A. Hameed, R. Binyamin: supervision, statistics, data analysis, project administration, and manuscript revision. M. Usman: CQD synthesis, characterization and lab assistance. M. Faisal, W. Hassan and MW Alam: methodological support and lab assistance. S. Ali: data analysis, interpretation, and manuscript editing.

***Acknowledgment*:** We are thankfull the Diagnostic Laboratory, MNS University of Agriculture, Multan, for laboratory space, equipment access, and technical assistance.

REFERENCES

Aftab, M., H. Ali, M. Ullah, S. Ikram, S.U. Khan, A. Wahab and M. Naeem. 2025. Biomedical Applications of Carbon Dots: Advances in Antimicrobial Therapy and Targeted Delivery Systems. Biomedical Materials & Devices 4:3136-3157.

Arshad, U., D. Chen, H. Cao, C. Feng, L. Liu, M.A. Ali, Z. Wanhong, Y. Li, L. Jiang and J. Yang. 2025. Biobased carbon quantum dots: An emerging nano-enabled paradigm for pesticide removal and sustainable plant protection. Science of the Total Environment 998:180290.

Balouiri, M., M. Sadiki and S.K. Ibnsouda. 2016. Methods for in vitro evaluating antimicrobial activity: A review. Journal of Pharmaceutical Analysis 6:71-79.

Dey, S., S. Hassan and R.K. Pandey. 2024. Nanomedicine in Targeted Drug Delivery: Precision Therapeutics for Personalized Medicine. In: V. Gautam, R. Kumar, K. Das Manandhar and S.C. Kamble (eds.), Nanomedicine. Springer Nature Switzerland, Cham. pp.179-231.

Kayani, K., D. Ghafoor, S. J. Mohammed and O.B. A. Shatery. 2024. Carbon dots: synthesis, sensing mechanisms, and potential applications as promising materials for glucose sensors. Nanoscale Advances 7:42-59.

Hadwan, M.H., A.H. Alta'ee, R.M. Mohammed, A.M. Hadwan, H.S. Al-Kawaz and Z.A. Al Talebi. 2024. An efficient protocol for quantifying catalase activity in biological samples. Bulletin of the National Research Centre 48:34.

Hameed, A., M. Zeeshan, R. Binyamin, M.W. Alam, S. Ali, M.S. Zaheer, H. Ali, M.W. Riaz, H.H. Ali and M.S. Elshikh. 2024. Molecular characterization of Pectobacterium atrosepticum infecting potato and its management through chemicals. PeerJ 12:e17518.

Haque, M.M., G.C. Das, Md.M. Faysal, M.A. Hossain, M. Haque, S. Miah, J. Farthouse, M. Rahman and Md.N.H. Mehedi. 2025. PCR-based detection technique and gamma irradiation strategies for managing *Ralstonia solanacearum* -induced brown rot of potato. International Journal of Radiation Biology 101:382-390.

Hu, J., C. Gong, Y. Jia, H. Feng, J. Chen, G. Qin, A. Liang, A. Peng, Y. Huang, M. Sun, H. Rao and X. Wang. 2024. Preparation of pH-responsive Kas@ZnO quantum dots for synergistic control of rice blast and enhanced disease resistance in rice. ACS Applied Materials and Interfaces 16:60842-60855.

Kumar, N., K. Tripathi and Y. Srivastava. 2025. Composition, optimization, and preparation of culture media for microbiological and biotechnological. *Biotechnology Lab Techniques:* Culture Media, Microscopy, and Microbial Analysis 13:19.

Marković, Z.M., D.D. Milivojević, J. Kovač and B.M. Todorović Marković. 2024. Phloroglucinol-based carbon quantum dots/polyurethane composite films: How structure of carbon quantum dots affects antibacterial and antibiofouling efficiency of composite films. Polymers 16:1646.

Mikhail, M.S., A.I. Abd-Alim, N.M. Balabel and A.M. Abbas. 2025. Evaluation of the antibacterial activity of some plant essential oils against Ralstonia solanacearum and the molecular diagnosis of the bacterium. Egyptian Pharmaceutical Journal 24:207-215.

Murei, A., W.B. Ayinde, M.W. Gitari and A. Samie. 2020. Functionalization and antimicrobial evaluation of ampicillin, penicillin and vancomycin with Pyrenacantha grandiflora Baill and silver nanoparticles. Scientific Reports 10:11596.

Packialakshmi, J.S. and J.T. Kim. 2025. Antimicrobial Mechanisms Exhibited by Carbon Quantum Dots. In: [Editor(s)] (ed./eds.), Carbon Quantum Dots from Natural Sources. CRC Press, Boca Raton, FL. pp.100-115.

Pei, S., Y. Wang, S. Cai, K. Yan, K. Luo and Y. Ma. 2025. Synthesis of sulfur-doped carbon quantum dots from Solanum nigrum for ciprofloxacin detection in yogurt samples and antibacterial activity. RSC Advances 15:27294-27299.

Rodríguez-Parra, J.A., J.P. Moreno-López and A. González-Almario. 2022. *Dickeya solani, Pectobacterium atrosepticum* and *Pseudomonas asplenii* : causal agents of bacterial soft rot in cyclamen plants (*Cyclamen persicum* Mill.) in Colombia. Canadian Journal of Plant Pathology 44:485-503.

Roostaee, M. and R. Ranjbar-Karimi. 2025. Emerging trends in carbon quantum dots: Synthesis, characterization, and environmental photodegradation applications. Materials Science in Semiconductor Processing 188:109212.

Shyntum, D.Y., N.P. Nkomo, N.L. Shingange, A.R. Gricia, D. Bellieny-Rabelo and L.N. Moleleki. 2019. The Impact of Type VI Secretion System, Bacteriocins and Antibiotics on Bacterial Competition of *Pectobacterium carotovorum* subsp. brasiliense and the Regulation of Carbapenem Biosynthesis by Iron and the Ferric-Uptake Regulator. Frontiers in Microbiology 10:2379.

Steel, R.G.D., J.H. Torrie and D.A. Dickey. 1997. Principles and Procedures of Statistics: A biometrical approach, 3rd Ed. McGraw-Hill Book Co., New York, USA

Thakur, R. 2024. Management of bacterial leaf blight of rice caused by Xanthomonas oryzae using organic approaches. M.Sc. (Hons.) Agriculture (Microbiology) Thesis. Division of Microbiology, Faculty of Basic Sciences, Sher-e-Kashmir University of Agricultural Sciences and Technology of Jammu, India.

Ton, T.P., R. Bright, V.K. Truong and K. Vasilev. 2025. Fluorescent Antibiotics: Bridging Diagnostic and Therapy in the Fight against Bacterial Infections. Small Science 5:2500138.

Usman, M., Y. Zaheer, M.R. Younis, R.E. Demirdogen, S.Z. Hussain, Y. Sarwar, M. Rehman, W.S. Khan and A. Ihsan. 2020. The effect of surface charge on cellular uptake and inflammatory behavior of carbon dots. Colloid and Interface Science Communications 35:100243.

Wang, S., D. Wang, G. Wang, M. Zhang, Y. Sun and J. Ding. 2024. Antibacterial carbon dots. Materials Today Bio 30:101383.

Weng, L., Z. Tang, M.F. Sardar, Y. Yu, K. Ai, S. Liang, J. Alkahtani and D. Lyv. 2024. Unveiling the frontiers of potato disease research through bibliometric analysis. Frontiers in Microbiology 15:1430066.

Yaish, M.W. 2024. Isolation and Identification of Growth-Promoting Bacteria from Plants Growing Under Abiotic Stresses. In: R. Sunkar (ed.), *Plant Stress Tolerance*. Springer US, New York, NY. pp.241-256.

Zhang, L., Y. Duan, S. Zhao, N. Xu and Y-Progress and Application. Animals 14:2659.

Zhou, R., W. Guo, J. Wang, X. Yu and Y. Wu. 2024. N-doped silicon QDs: facile synthesis and application as sensor for discrimination and selective detection of oxytetracycline, tetracycline, and chlortetracycline in foods. Microchimica Acta 191:698.